LASERS

Frequency locking of a semiconductor laser by a ring fibre resonator

Quantum Electronics **47** (10) 871–876 (2017)

LASERS

https://doi.org/10.1070/QEL16449

Frequency locking of a semiconductor laser by a ring fibre resonator

I.O. Zolotovskii, D.A. Korobko, A.A. Fotiadi, K. Panajotov

Abstract. **We propose a model for the oscillation of a single-frequency feedback semiconductor laser based on a ring fibre interferometer. It is shown that at a certain level of feedback, the semiconductor laser generation frequency is locked by the transmission peak of the fibre interferometer. The effect is accompanied by the narrowing of the spectral line and the reduction of noises. The described results are in qualitative agreement with the experimental data.**

Keywords: *frequency locking, ring fibre resonator, semiconductor laser.*

1. Introduction

Stabilisation and narrowing of the oscillation line in semiconductor lasers attract significant interest because of a large number of potential applications. Among them are the coherent optical communication, distributed monitoring systems and microwave photonics applications [1–4]. One of the most promising mechanisms of line narrowing of semiconductor laser radiation is the frequency locking by means of the feedback throug an external cavity [5]. This relatively simple method allows the design of inexpensive narrow-band light sources based on standard diode lasers, which favourably distinguishes it from the use of active feedback systems.

A traditional scheme of frequency locking comprises a narrow-band optical filter in a weak feedback loop. In recent years the solutions have been actively studied, in which the role of the optical filter is played by a whispering-gallery-mode microresonator [6–11]. This scheme has been reported to allow the linewidth on the order of 1 Hz to be reached [11], but its certain drawback is the limited possibility of tuning the parameters. An alternative way is to use all-fibre schemes with an external resonator of increased length, but less Q-factor, e.g., the feedback loops based on an external ring resonator [12, 13]. Using the standard fibre components, this approach allowed similar values of the linewidth at essentially softer requirements to the elements of the system implemented in cheaper configurations. Such solutions are particularly promising for further development of double-frequency radiation sources, relevant in the problems of distributed monitoring, RF spectrometry, etc. In this case, the narrow-band radiation of the diode laser trapped in the fibre resonator efficiently generates the Brillouin signal, and the frequency difference between the pump and the Stokes Brillouin component is constant and equal nearly to 11 GHz for a standard silica fibre [14, 15]. Thus, the study of diode lasers with the above type of feedback is of significant interest for applications.

At the same time it is worth noting that semiconductor lasers with feedback are complex dynamic systems, demonstrating a variety of states – from steady-state oscillation, periodic and quasi-periodic pulsations to the chaotic oscillation regime [16–20]. Although their dynamics is studied well enough, including the case of feedback via a frequency filter [21, 22], the papers on the dynamics of a semiconductor laser oscillation with a ring resonator feedback are unknown to us. A specific feature of this type of feedback is the presence of periodic jumps of the oscillation frequency [13, 14] that limit the stability of laser operation. The aim of the present paper is the theoretical study and simulation of the dynamics of semiconductor laser oscillation with a ring resonator feedback. In our opinion, the issue is urgent, and the results are expected to provide at least qualitative explanation of the experimental observations.

2. Model

Figure 1 illustrates the system consisting of a semiconductor laser and a ring fibre resonator, connected to form a feedback loop. The standard model of a semiconductor Fabry–Perot laser (FPL) is considered. Further calculations are valid also for a semiconductor distributed feedback (DFB) laser in the approximation that the reflection coefficient of the FPL output mirror is correlated with the coupling coefficient σL in the periodic structure of the DFB laser (thus, the reflection coefficient of the FPL external mirrors $R = 0.32$ corresponds to the DFB coupling coefficient $\sigma L = 2.2$ [17]).

The considered frequency range is limited by a few resonances of the ring interferometer a few metres long, which corresponds to the spectral bandwidth up to tens of GHz. The characteristic roundtrip time τ_L for the FPL amounts to a few picoseconds. For the DFB laser with a resonator of the same length this value is somewhat smaller, but close by the order of magnitude. The free spectral range (FSR) of the semiconductor laser is $1/\tau_L > 100$ GHz (here we neglect the fact that the DFB laser modes are not equidistant). Thus, only one lon-

I.O. Zolotovskii, D.A. Korobko Ulyanovsk State University, ul. L.Tolstogo 42, 432700 Ul'yanovsk, Russia;
e-mail: razfol.14@mail.ru, korobkotam@rambler.ru;
A.A. Fotiadi University of Mons (Belgium), 20, place du Pare, B7000 Mons, Belgium; Ulyanovsk State University, ul. L.Tolstogo 42, 432700 Ul'yanovsk, Russia; e-mail: fotiadi@mail.ru;
K. Panajotov Brussels Photonics Team, Department of Applied Physics and Photonics (B-PHOT TONA), Vrije Universiteit Brussel, Pleinlaan 2, 1050 Brussels, Belgium

Received 8 June 2017; revision received 13 July 2017
Kvantovaya Elektronika **47** (10) 871–876 (2017)
Translated by V.L. Derbov

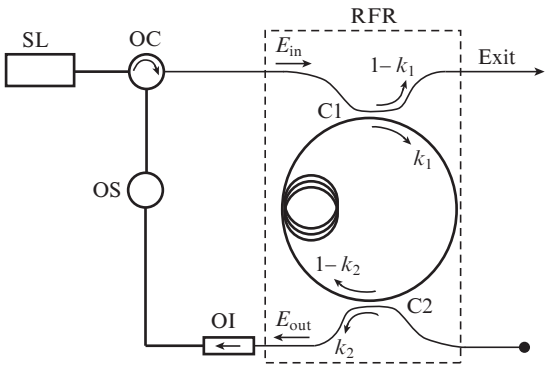

Figure 1. Schematic of a semiconductor laser with feedback through a ring fibre resonator:
(SL) semiconductor laser; (OC) optical circulator; (RFR) ring fibre resonator; (OS) optical switch (allowing feedback loop opening); (C1, C2) couplers with the division coefficients k_1 and k_2, respectively; (OI) optical insulator.

gitudinal mode is of interest, which possesses the maximal gain and the minimal lasing threshold. In this sense, the considered semiconductor laser can be referred to as a single-frequency one. It should be also noted that the effects related to the polarisation of radiation are not taken into account, i.e., the radiation field is considered to be linearly polarised, and all elements (insulator, couplers) are polarisation-maintaining.

To study the lasing dynamics, we used the standard system of Lang–Kobayashi equations for a semiconductor laser with feedback. The equations describe the variation of the number S of photons, the phase φ and the number of charge carriers n [23]:

$$\frac{\mathrm{d}S}{\mathrm{d}t} = \left[G(n-n_0) - \frac{1}{\tau_\mathrm{p}}\right]S + Q + 2k_\mathrm{c}\sqrt{f_\mathrm{ext}}\sqrt{S(t)\,S(t-\tau_0)}$$

$$\times\cos[\omega_0\tau_0 + \varphi(t) - \varphi(t-\tau_0)] + F_S(t),$$

$$\frac{\mathrm{d}\varphi}{\mathrm{d}t} = \frac{1}{2}\alpha G(n-n_\mathrm{th}) - k_\mathrm{c}\sqrt{f_\mathrm{ext}}\sqrt{\frac{S(t-\tau_0)}{S(t)}}$$

$$\times\sin[\omega_0\tau_0 + \varphi(t) - \varphi(t-\tau_0)] + F_\varphi(t), \qquad (1)$$

$$\frac{\mathrm{d}n}{\mathrm{d}t} = \frac{I-I_\mathrm{th}}{e} - \frac{n}{\tau_\mathrm{s}} - G(n-n_0)\,S + F_n(t).$$

Here τ_0 is the feedback delay time;

$$k_\mathrm{c} = \frac{1}{\tau_L}\frac{1-R}{\sqrt{R}} \qquad (2)$$

is the parameter determined by the reflection coefficient of the semiconductor laser mirror R and the effective time of resonator roundtrip $\tau_L = 2n_\mathrm{ref}L_D/c$; f_ext is the fraction of power extracted to the resonator; $\omega_0 = \mathrm{d}\varphi/\mathrm{d}t|_{n-n_\mathrm{th}}$ is the centre frequency of the semiconductor laser oscillation at the lasing threshold in the absence of feedback; α is the spectral broadening coefficient of the semiconductor; $I - I_\mathrm{th}$ is the difference between the operating current and the threshold one; e is the elementary charge; τ_s is the carrier lifetime; τ_p is the photon lifetime; the gain $g = G(n-n_0)$ is written in the linear approximation relative to the number of nonequilibrium carriers (n_0 is the number of nonequilibrium carriers, corresponding to a zero gain); n_th is the number of nonequilibrium carriers corresponding to the lasing threshold; $Q = \beta/\tau_\mathrm{p}$ describes the spontaneous emission (β is the inversion coefficient); and F_i denotes the Langevin noise forces with a Gaussian distribution, introduced in a standard way (as in Ref. [24]) and calculated using the generator of random numbers. The values of parameters used in the simulation are typical for semiconductor lasers and presented below.

Length of semiconductor laser resonator L_D/μm	300
Refractive index of the semiconductor n_ref	3.53
Spectral broadening coefficient α	5
Lifetime of charge carriers τ_s/ns	2
Photon lifetime τ_p/ps	4
Mirror reflection coefficient R	0.32
Number of nonequilibrium carriers, corresponding to a zero gain, n_0	10^8
Differential gain G/s^{-1}	10^4
Inversion coefficient β	2.2
Radiation wavelength, corresponding to the centre of the free laser spectrum at the lasing threshold $\lambda_0 = 2\pi c\omega_0^{-1}$/nm	1550
Threshold current I_th/mA	15
Operating current I/mA	17

By solving system (1), one can analytically express the quantities S_th and n_th, corresponding to the lasing threshold, i.e., the steady-state values (in the absence of noises) of the radiation characteristics of an isolated semiconductor laser. Further solution of the obtained model system of nonlinear equations was performed numerically using the fourth-order Runge–Kutta method. The spectral characteristics were determined by means of the Fourier transform of the temporal dependence $E(t) = \sqrt{S(t)}\exp[\mathrm{i}\varphi(t)]$. In the absence of feedback, the time-averaged oscillation parameters (the mean value of carriers $\langle n\rangle$, the mean number of photons $\langle S\rangle$, and the mean frequency $\omega = \langle \mathrm{d}\varphi/\mathrm{d}t\rangle$ are determined by the values of the operating current I and can be found from the steady-state solution of Eqns (1), taking into account that $f_\mathrm{ext} = 0$ and the Langevin noise forces are independent Gaussian processes with a zero mean value. The numerical solution of Eqns (1) in this case shows that the laser possesses the spectral linewidth ~10 MHz. Figure 2a shows typical spectral lines of the semiconductor laser oscillation without feedback and the spectrum obtained by averaging ten different lines, corresponding to different independent noises. Its width amounts to about 9 MHz at a level of 3 dB from the maximal value.

It follows from Eqns (1) that the feedback switch-on leads to the change in the threshold gain level and the oscillation frequency of the semiconductor laser, determined by the fraction of power f_ext extracted to the laser cavity and the feedback phase. Neglecting the noise forces it is possible to derive the following equations for the oscillation frequency of the laser with feedback $\omega = \mathrm{d}\varphi/\mathrm{d}t$ (often referred to as the mode frequency of the external cavity) and the change of the gain threshold Δg [16, 17, 23]:

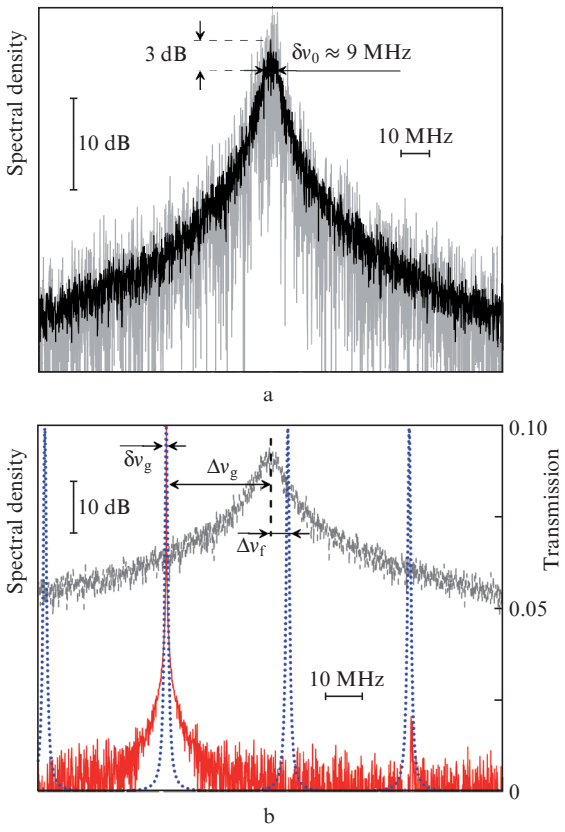

Figure 2. (a) Spectrum of a semiconductor laser without feedback (the grey background is a typical lasing line, the black spectrum is obtained by averaging over ten different lines) and (b) example of semiconductor laser stabilisation with a feedback ring interferometer having a length L_r = 4 m and transmission $l_{ext} = 4 \times 10^{-4}$ (the background is the averaged spectrum of a free semiconductor laser; the dashed line shows the transmission $|k_{ext}|^2$ of the ring interferometer).

$$(\omega - \omega_0)\tau_0 = -C\sin(\omega\tau_0 + \arctan\alpha),$$
$$\Delta g = -2k_c\sqrt{f_{ext}}\cos(\omega\tau_0), \qquad (3)$$

where the parameter $C = k_c\tau_0\sqrt{f_{ext}(1+\alpha^2)}$ is called the reduced feedback coefficient. From the analysis of the stability of system (1) with respect to small perturbations one can derive the expression for the lasing linewidth $\delta\nu_g$, which is related to the free laser linewidth $\delta\nu_0$ as $\delta\nu_g \sim \delta\nu_0/[1 + C \times \cos(\omega\tau_0 + \arctan\alpha)]^2$ [16, 17, 23]. These expressions provide the base for the principle of stabilisation and narrowing the line of the semiconductor laser by means of feedback. Depending on the value of the parameter C, it is possible to describe several scenarios. For $C < 1$, the linewidth is mainly determined by the phase of the feedback $\omega\tau_0$ (regime I). With the growth of f_{ext} in the transient regime ($C \geqslant 1$), the line narrowing is observed (regime II). With a further increase in f_{ext} ($C \gg 1$) one observes the frequency locking determined by the condition $\omega\tau_0 = 2\pi - \arctan\alpha$. In this case, the linewidth is minimal (regime III). The latter scenario is limited by a certain value of f_{ext}, exceeding which we arrive at the so-called collapse of coherence, accompanied by a significant broadening of the lasing line (regime IV) [16].

A specific feature of the present paper is the consideration of resonance in the feedback loop. In contrast to the studies considering the feedback analysis with a Lorentz frequency filter [21], we consider a frequency filter with multiple transmission lines, corresponding to the transmission through the ring fibre resonator. The amplitude reflection coefficient of the ring resonator $k_{ext}(\omega)$ relates the amplitudes of the radiation entering the ring interferometer and transmitted through it, namely, $E_{out} = k_{ext}E_{in}$ (see Fig. 1). Therefore, this coefficient determines the fraction $f_{ext} = |k_{ext}|^2 l_{ext}$ of the power extracted to the resonator, where l_{ext} is the transmission taking the losses in the feedback loop into account. In particular, they include the losses of about 30 dB at the optical insulator installed at the output of the majority of present-day semiconductor lasers to prevent the unwanted feedback. The reflection coefficient of the resonator can be expressed as [13]

$$k_{ext}(\omega) = \frac{\sqrt{(1-\gamma_1)k_1k_2}\exp(i\omega\tau_r)}{\sqrt{\delta(1-\gamma_1)(1-k_1)} - \exp(i\omega\tau_r)}, \qquad (4)$$

where k_1, k_2 are the division coefficients of the couplers; $\delta = (1-k_2)\times 10^{-(\zeta+\gamma_2)/10}$ is the coefficient of power transmission through the ring resonator (dB), determined by the losses in the output coupler and the losses ζ in the fibre connections of the ring interferometer (the losses in the fibre are neglected); γ_1, γ_2 are the loss coefficients in the couplers; and τ_r is the delay time in the ring resonator. The parameters of the ring resonator corresponding to the coupling regime close to the critical one [13] are presented below.

Length of the ring resonator L_r/m	4
Length of the connecting fibre L_{con}/m	2.56
Fibre refractive index n_f	1.5
Feedback transmission l_{ext}	$0–4 \times 10^{-4}$
Division coefficient k_1	0.1
Division coefficient k_2	0.01
Losses in the couplers γ_1, γ_2/dB	0.1
Losses of power in the ring resonator δ/dB	0.35

In order to consider the feedback resonance, the appropriate terms in Eqns (1) should be rewritten as convolutions, corresponding to the response after the transmission through the ring interferometer. Thus, the second terms in the right-hand sides of the first and the second equation of system (1) take the form

$$k_c\sqrt{l_{ext}}\int_0^{t-\tau_0-\tau_r} d\tau\,|k_{ext}(\tau)|\sqrt{S(t)S(t-\tau_0-\tau_r-\tau)}\times$$
$$\times\cos[\omega_0(\tau_0+\tau_r+\tau)+\varphi(t)-\varphi(t-\tau_0-\tau_r-\tau)+\arg(k_{ext}(\tau))],$$
$$k_c\sqrt{l_{ext}}\int_0^{t-\tau_0-\tau_r} d\tau\,|k_{ext}(\tau)|\sqrt{S(t-\tau_0-\tau_r-\tau)/S(t)}$$
$$\times\sin[\omega_0(\tau_0+\tau_r+\tau)+\varphi(t)-\varphi(t-\tau_0-\tau_r-\tau)+\arg(k_{ext}(\tau))].$$

Here $\tau_0 = n_f L_{con}/c$ is the delay time in the connecting fibre; $\tau_r = n_f L_r/c$ is the delay time in the ring interferometer; n_f is the refractive index of the fibre; and $k_{ext}(\tau)$ is the source function of the feedback, given by the inverse Fourier transform of $k_{ext}(\omega)$. This function differs from zero only for the moments of time, corresponding to the full roundtrip of the ring interferometer $\tau = m\tau_r$, $m = 0, 1, \ldots, +\infty$.

3. Results and discussion

Figure 2b shows a typical example of radiation stabilisation for the above parameters. For the simulation, the difference between the nearest resonance of the interferometer and the threshold frequency $\omega_0/2\pi$ was specified as $\Delta\nu_f = 8.5$ MHz. However, one can see that the feedback is implemented using another resonance of the interferometer. Because of the threshold reduction and the oscillation frequency shift, the transmission peak with a lower frequency becomes preferable for the laser feedback. The difference between the oscillation frequency of the laser with feedback and the threshold frequency $\omega_0/2\pi$ is denoted by $\Delta\nu_g$. In the present case, $\Delta\nu_g = -41$ MHz. The lasing linewidth $\delta\nu_g$ at the level of 3 dB from the maximum is less than 20 kHz. Thus, the line is narrowed by more than 450 times. It is worth noting that the accuracy of calculations is limited by the simulation time. To represent the spectrum, 2^{19} points were calculated with a step 50 ps, which provided a frequency step $d\nu \approx 40$ kHz. The enhancement of accuracy is associated with a significant growth of computing expenditures, and in the present paper it is limited by a step $d\nu/2 \approx 20$ kHz.

From Fig. 2b it is seen that the reduction of the lasing threshold occurs only at a particular peak of the interferometer transmission, for which the constructive interference takes place in the resonator of the semiconductor laser between the field generated in the resonator and the feedback radiation. At the frequencies corresponding to the adjacent resonances of the interferometer, the destructive interference takes place, increasing the lasing threshold. For the rest of the frequency range the threshold is constant, which finally leads to the reduction of the relative noise level. In particular, in the presented example the level of noise is reduced by more than 30 dB.

Now let us consider the change of the laser spectral characteristics under the variation of the feedback level (Fig. 3). Figure 3a shows the change of the lasing line for the feedback increasing from $l_{ext} = 6.25 \times 10^{-6}$ to 4×10^{-4}. Note that for weak feedback ($l_{ext} = 6.25 \times 10^{-6}$), the spectrum of the free laser is distorted, but the reduction of threshold is insufficient for suppressing the oscillation near the free laser centre frequency. The spectral distortions arise near the frequencies corresponding to the modes of the ring interferometer. In the region closest to the mode centre, the destructive interference occurs with increasing the lasing thresholds, which leads to the formation of an intensity dip. Near the adjacent mode, the threshold is reduced (the constructive interference occurs), but the feedback is insufficient for shifting the lasing frequency to this region. On the contrary, the maximum of lasing shifts to the zone of the nearest mode of the interferometer, but demonstrates nonresonance behaviour.

When the feedback is increased to $l_{ext} > 2 \times 10^{-5}$, the lasing line shifts to the region of constructive interference and becomes attached to the transmission peak of the interferometer (See Fig. 3a). Note that with an increase in the feedback, the lasing is stabilised, i.e., the linewidth narrows and the level of background noise decreases. From Fig. 3.b one can see that with an increase in the feedback from $l_{ext} = 1 \times 10^{-4}$ to 4×10^{-4}, alongside with the line narrowing, the lasing frequency becomes fixed at the interferometer transmission peak. One can treat this effect as the lasing line locking. With a further growth of the feedback ($l_{ext} > 5 \times 10^{-4}$), we observed the excitation of multiple additional modes of the

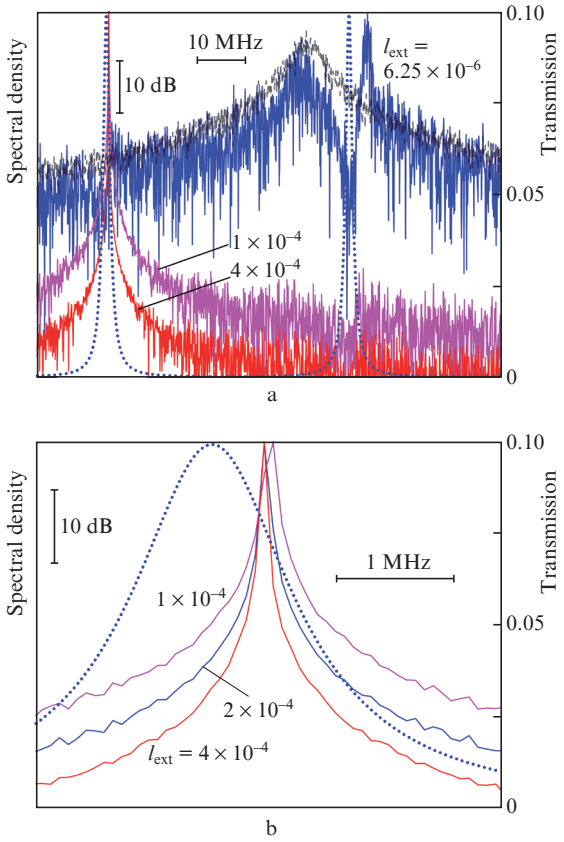

Figure 3. (a) Laser spectra for different level of feedback, as well as the free laser spectrum and the transmission $|k_{ext}|^2$ of the ring interferometer (dotted curve). (b) The same in a larger scale near the transmission peak $|k_{ext}|^2$.

ring interferometer and the lasing line broadening, i.e., the phenomena typical for the 'coherence collapse'. In the present paper these phenomena are not considered, that is why the maximal level of feedback is restricted to the value of $l_{ext} = 1 \times 10^{-4}$. Below we assume that the feedback is at this level.

Finally, let us consider the specific feature of the laser line locking by changing the detuning $\Delta\nu_f$ between the free laser spectrum centre and the nearest resonance of the interferometer. Physically this situation can correspond to temperature variations of the ring resonator length or current modulation in the semiconductor laser. Figure 4a presents the oscillation lines of the laser with feedback, obtained at different detunings $\Delta\nu_f$. As seen from the Figure, due to the resonance dependence $f_{ext}(\omega)$, small variations of $\Delta\nu_f$ give rise to small variations of the lasing frequency $\Delta\nu_g$, i.e., within certain limits the lasing line follows the variations of the frequency of the ring interferometer transmission peak. However, it is necessary to note that the frequency shift of the constructive interference differs from the shift $\Delta\nu_f$, i.e., the lasing frequency changes its position within the transmission peak, which occurs due to the nonlinear dependence of the frequency change $\Delta\nu_g$ on the magnitude of the feedback (3).

The main result of the present paper is shown in Fig. 4b, demonstrating the lasing frequency change as a function of detuning $\Delta\nu_f$. It is worth noting that the size of the continuous regions of the lasing frequency locking amount to nearly 10 MHz, so that during the variation of the detuning within a

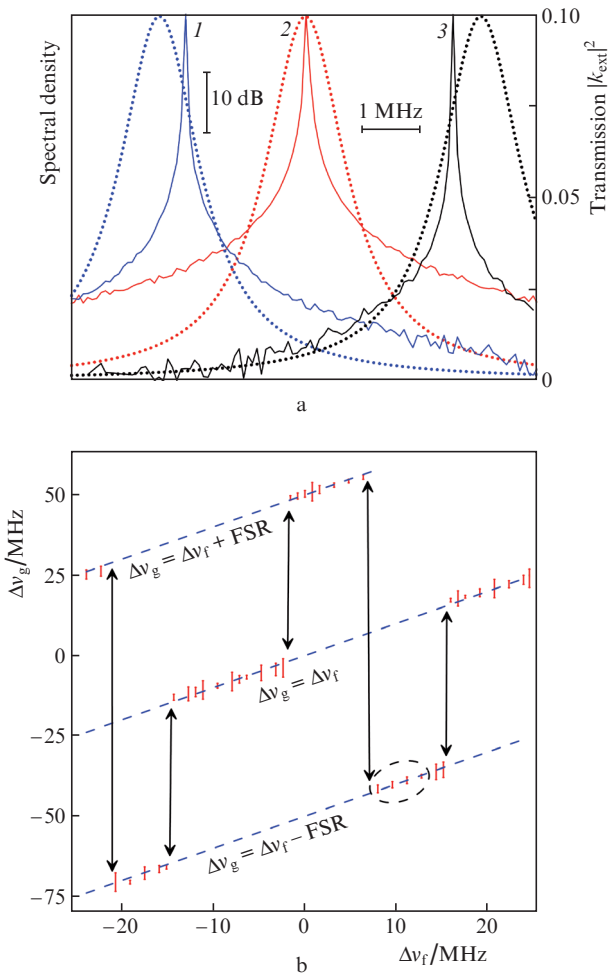

Figure 4. (a) Oscillation lines of the laser with feedback and the transmission of the individual resonance of the ring interferometer (dotted curves) for the detuning $\Delta\nu_f$ = (*1*) 8.4, (*2*) 11 and (*3*) 14 MHz, as well as (b) change in the lasing frequency in the presence of feedback as a function of $\delta\nu_g$ at the 3 dB level (the scale 30:1). The dashed lines show the change in the frequencies of three peaks of the ring interferometer absorption with the free spectral parameter FSR = $n_f L_r/c$, the arrows show the jumps of the lasing lines. The region corresponding to Fig. 4a is also shown.

single region the lasing frequency varies continuously, remaining attached to a definite transition peak of the ring interferometer. Therefore, under the essential temperature fluctuations or modulations of the injection current, the mechanism of steady-state oscillation with feedback is maintained, permanently tuning the lasing frequency and, as a rule, conserving the linewidth. The lasing linewidth is determined by the shape of the potential well, related to the transmission peak of the interferometer, in which the dynamical system with feedback turns out to be [25, 26].

The noise destroys the constrictive interference tuning and leads to the broadening of the lasing line. Note that at some values of the detuning $\Delta\nu_f$ the situation of an equivalent choice between the feedback channels. In this case the noise can induce a jump between the modes of the ring interferometer, which leads to a jump of the lasing frequency by the integer multiple of the free spectral parameter of the interferometer FSR = $n_f L_r/c$. The stochastic frequency jumps obviously limit the laser stability and worsen its characteristics. Therefore, in order to provide stable oscillation it is technically important to support thermal stability and reduce the noise modulation of power supply.

4. Conclusions

We present an oscillation model for a single-frequency semiconductor laser with feedback using a ring fibre interferometer. It is shown that at a certain level of feedback, the oscillation frequency of the semiconductor laser is locked by the transmission peak of the fibre interferometer, which is accompanied by the spectral line narrowing and the noise level reduction. It is also found that with changing the parameters of the system leading to a shift of the interferometer transmission peaks with respect to the oscillation frequency of the free semiconductor laser (variations of fibre length, current modulation), the lasing frequency with feedback continuously varies within a certain range, staying within the transmission peak. Moreover, it is established that under certain detunings of the transmission peak from the free laser oscillation frequency, the lasing frequency undergoes a jump related to a change of the feedback channel. The described effects are in qualitative agreement with the data of the experiments [13, 14]. The practical importance of the present paper relates to the fact that the presented model makes it possible to develop the theory of narrowband double-frequency lasers with a ring fibre resonator, in which the locked-in frequency of the semiconductor laser serves to pump the Brillouin signal [14, 15]. The development of such lasers is extremely promising for spectroscopic applications, distributed monitoring, etc.

Acknowledgements. The work was supported by the Ministry of Education and Science of the Russian Federation (Project No. 14.Z50.31.0015, State Research Task No. 3.3889.2017) and by the Russian Foundation for Basic Research (Grant No. 16-42-732135 r_ofi_m).

References

1. Li Q., Yan F.P., Peng W.J., Yin G.L., Feng T., Tan S.Y., Liu S. *Opt. Laser Technol.*, **56**, 304 (2014).
2. Sotor J.Z., Dudzik G., Abramski K.M. *Opt. Commun.*, **291**, 279 (2013).
3. Babin S.A., Churkin D.V., Ismagulov A.E., Kablukov S.I., Nikulin M.A. *Laser Phys. Lett.*, **4**, 428 (2007).
4. Ge Y., Guo S., Han Y., Wang J. *Opt. Commun.*, **334**, 74 (2015).
5. Dahmani B., Hollberg L., Drullinger R. *Opt. Lett.*, **12**, 876 (1987).
6. Vasil'ev V.V., Velichansky V.L., Gorodetskii M.L., Il'chenko V.S., Holberg L., Yarovitsky A.V. *Quantum Electron.*, **26**, 657 (1996) [*Kvantovaya Elektron.*, **23**, 675 (1996)].
7. Vassiliev V.V., Velichansky V.L., Il'chenko V.S., Gorodetsky M.L., Hollberg L., Yarovitsky V.A. *Opt. Commun.*, **158**, 305 (1998).
8. Oraevsky A.N., Yarovitsky A.V., Velichansky V.L. *Quantum Electron.*, **31**, 897 (2001) [*Kvantovaya Elektron.*, **31**, 897 (2001)].
9. Vassiliev V.V., Il'ina S.M., Velichansky V.L. *Appl. Phys. B*, **76**, 521 (2003).
10. Liang W., Ilchenko V.S., Savchenkov A.A., Matsko A.B., Seidel D., Maleki L. *Opt. Lett.*, **35**, 2822 (2010).
11. Liang W., Ilchenko V.S., Eliyahu D., Savchenkov A.A., Matsko A.B., Seidel D., Maleki L. *Nature Commun.*, **6**, 7957 (2015).
12. Spirin V.V., Castro M., López-Mercado C.A., Mégret P., Fotiadi A.A. *Laser Phys.*, **22**, 760 (2012).
13. López-Mercado C.A., Spirin V.V., Bueno Escobedo J.L., Lucero A.M., Mégret P., Zolotovskii I.O., Fotiadi A.A. *Opt. Commun.*, **359**, 195 (2016).
14. Spirin V.V., López-Mercado C.A., Mégret P., Fotiadi A.A. *Laser Phys. Lett.*, **9**, 377 (2012).

15. Spirin V.V., López-Mercado C.A., Kablukov S.I., Zlobina E.A., Zolotovskiy I.O., Mégret P., Fotiadi A.A. *Opt. Lett*., **38**, 2528 (2013).
16. Ohtsubo J. *Semiconductor Lasers: Stability, Instability and Chaos* (Berlin: Springer, 2012).
17. Petermann K. *Laser Diode Modulation and Noise* (Berlin: Springer Science & Business Media, 2012).
18. Napartovich A.P., Sukharev A.G. *Quantum Electron*., **34**, 630 (2004) [*Kvantovaya Elektron*., **34**, 630 (2004)].
19. Sukharev A.G., Napartovich A.P. *Quantum Electron*., **37**, 149 (2007) [*Kvantovaya Elektron*., **37**, 149 (2007)].
20. Napartovich A.P., Sukharev A.G. *Quantum Electron*., **45**, 193 (2015) [*Kvantovaya Elektron*., **45**, 193 (2015)].
21. Yousefi M., Lenstra D., Vemuri G. *Phys. Rev. E*, **67**, 046213 (2003).
22. Erzgräber H., Krauskopf B., Lenstra D., Fischer A.P.A., Vemuri G. *Phys. Rev. E*, **73**, 055201 (2006).
23. Schunk N., Petermann K. *IEEE J. Quantum Electron*., **24**, 1242 (1988).
24. Schunk N., Petermann K. *IEEE J. Quantum Electron*., **22**, 642 (1986).
25. Mork J., Tromborg B. *IEEE Photon. Technol. Lett*., **2**, 21 (1990).
26. Lenstra D. *Opt. Commun*., **81**, 209 (1991).